2P2-6

Development and evaluation of automated abdominal sound speed tomographic imaging system

腹部音速トモグラフィー自動画像化システムの開発と評価

Akira Yamada[1†], Kensuke Kawai[1], and Tomohiro Kurokawa[1] ([1]Grad.Bio-Appl.Sys. Eng., Tokyo Univ. of A&T)

山田 晃[1†], 河井健輔[1], 黒川智大[1] ([1]東京農工大学 院生物シ応用)

1. Introduction

We have been studying to realize abdominal cross section visceral fat test based on ultrasonic tomography method. [1],[2],[3] The method reproduces abdominal cross sectional sound velocity image information by applying tomography method to sound wave travel time data observed by mechanically scanning the sound wave transceiver around the abdomen. For the development of automated system being available in clinical use, an open-air type abdominal body surface scanning machinery was introduced. In practical application of the system, however, problems to be solved remained. For instance, introduction of tracking mechanism is inevitable to follow the human body motion. In addition, practicality of the method regarding the deteriorations caused by transmission through the spine or the intestinal gas is unclear. In the present study, the investigations are made regarding to these issues, and results of the validity verification experiments are demonstrated.

2. Method

2.1 Structure of automated abdominal body scanning system

Automated abdominal body scanning system as shown in Fig.1 was fabricated. The system includes facing pair of transducers (broad band piezoelectric circular plate with diameter 40 mm), pulsar /receiver (high voltage impulse generator, amplifier and AD converter), and automated actuating machinery for positioning of transducers to desired positions on the body surface. Here, facing pair of transmitter and receiver is attached on the tip of the actuators for pushing action (stroke 300 mm). For good transmission of ultrasound from transducers to the body, the couplers which are made of arum root and 40 mm radius hemisphere are putted in front of the transducers. The transmitter and receiver are individually mounted on the linear stages for translation action (stroke 600 mm). In addition, three laser range sensors (precision 50 um) are installed for the real time monitoring of body surface contour. The all units described above are mounted on a rotation ring

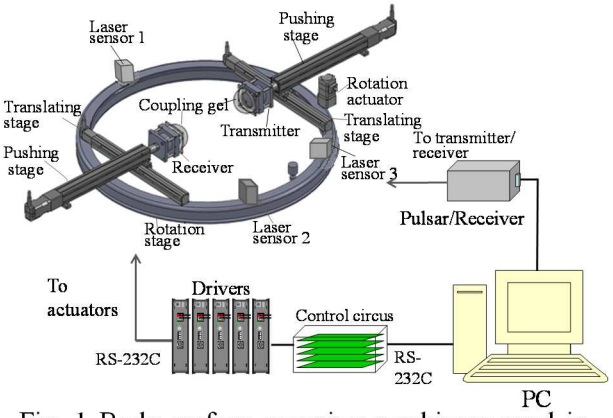

Fig. 1 Body surface scanning machinery used in the experiment.

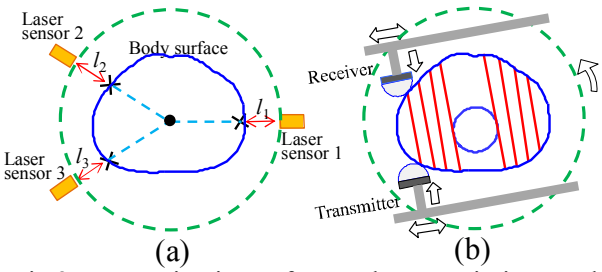

Fig.2 Determination of sound transmission and reception paths, (a) measurement of the body surface contour by laser range sensor, (b) translation scan avoiding the spine and calculation of the body surface contact point.

stage (diameter 720 mm). They are operated simultaneously by sending commands from the main personal computer.

2.2 Determination of transmission and reception paths avoiding the spine

As shown in Fig. 2(a), the body contour data measured by the laser range sensors are prepared beforehand for the estimation of the spine position and calculations of the transducer positions on the body surface. They are also used as the data for the real time monitoring of body motions in the middle of the sound wave measurements. After the preliminary preparation, sound wave travel time measurements are conducted by rotating transducers around body and contacting transducers against body surface, as shown in Fig. 2(b).

2.3 Real time body motion monitoring by three direction laser measurement

yamada@cc.tuat.ac.jp

If the body moves due to factors such as body swaying or respiratory stretching in the middle of the measurement, it becomes difficult to move the transceiver into contact with the intended body surface point. In order to avoid the difficulty, the body motions at the time of measurement are monitored in real time. For this purpose, as shown in Fig. 2(a), the distances l_1, l_2 and l_3 from three directions to the body surface are measured using laser range sensors located at three positions on the circumferential ring. Let $B(x,y)$ be the initial data of the body surface contour measured beforehand. The contour is deformed like $B(x-x_0, \alpha(y-y_0))$ due to the body motion. Here, (x_0,y_0) is a swaying translational displacement, and α is an respiratory expansion/contraction parameter. By determining the parameter x_0, y_0 and α that best fits to the measured distances l_1, l_2, l_3, the body surface contour after body movement can be obtained. Note that the body swaying occurs uniformly in every direction, on the other hand, respiratory displacement only on the ventral side. The fact makes it possible to discriminate the swaying displacement and respiratory stretching.

3. Test experiment

3.1 Real time body motion monitoring test

We performed body motion monitoring tests on actual human subject. An example of the temporal change of measured distances l_1, l_2, l_3 captured by three laser sensors during the measurement along one particular path with rotation angle 130 deg. are shown in Fig. 3. Here, the subject remained still in the first half time interval, after that swayed on purpose in the latter half, while taking natural breath all over the time. Due to the fact that respiratory stretching occurs only on the ventral side not on the back side, only the results measured by laser sensor 1 shows displacements in the first half time interval. In the latter half of time, the swaying motions were observed in all of the laser sensors.

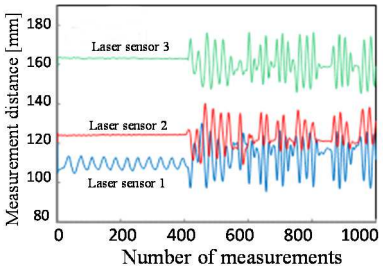

Fig. 3 Temporal change of body surface distance measured by three laser range sensors.

3.2 Determination of sound propagation paths and travel time measurement for human subject

An evaluation test was conducted on a human subject. Based on the preliminary measured body surface data, 146 numbers of paths were determined, where a circular spine region with radius 44 mm was avoided (position and size of the spine were roughly estimated in accordance with an X-ray CT image of the subject). By virtue of the detected body motion information, sound wave data were collected with a high degree of accuracy. Figure 4 shows the measured travel time data, where the results are compared between experiment (blue line) and simulation (red line). They are relatively in good agreement, to demonstrate that present automated system works fine as our expectation.

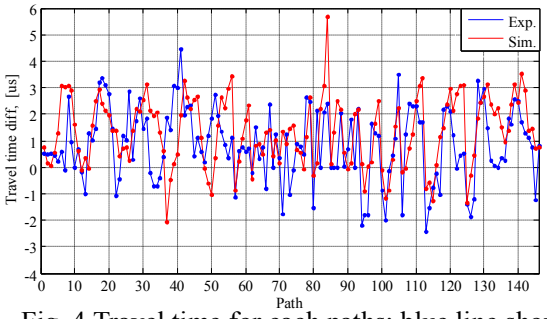

Fig. 4 Travel time for each paths: blue line shows experiment time data and red line shows simulation data.

3.3 Result of sound speed image reconstruction

Using the measured sound wave travel time data, sound speed image was reconstructed as shown in Fig. 5(a). In addition, reconstructed image using simulation data and X-ray CT image were compared as shown in Fig. 5(b) and (c). We can confirm that the result using the experiment data is close to the simulation. However, reproducibility of the peripheral area (such as stomach muscle and subcutaneous fat region) is not sufficient. We consider that degradation of the image is caused by the lack of sound wave path touching to the body surface. Hence, the image will be improved if the body surface vicinity data can be collected and included in the tomographic calculation.

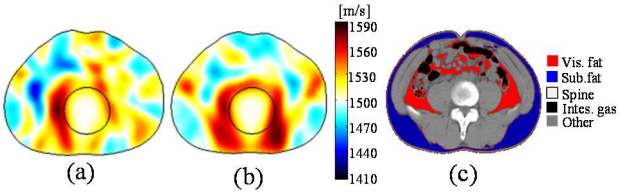

Fig. 5 Abdominal image of human subject, (a) reconstructed sound speed image using experiment data, (b)image using simulation data, (c)X-ray CT image.

References

1. K. Nogami, A. Yamada, Jpn.J.Appl.Phys., 46, pp.4820-4826 (2007).
2. T. Yokoyama, D. Shimizu and A. Yamada, Proc. Symp. Ultrasonic Electronics, 35, pp.449-450(2014).
3. A. Yamada, K. Kawai, and T. Kurokawa, Proc. Symp. Ultrasonic Electronics, 37 (2016).